Measurement and analysis of alpha-induced reactions on Ta, Ag and Co

M ISMAIL and A S DIVATIA

Variable Energy Cyclotron Centre, I/AF, Bidhan Nagar, Calcutta 700 064, India

Abstract. Excitation functions for the reaction ^{181}Ta (α, xn) $^{185-x}$Re, ^{107,109}Ag $(\alpha, ypxn)$ and ^{59}Co $(\alpha, ypxn)$ were obtained from measurements of residual activity of stacked foils from thresold to 60 MeV. The excitation functions for the production of ^{181}Re, ^{182}Re, ^{183}Re, ^{184}Re, ^{105}Ag, ^{111}In, ^{54}Mn, ^{56}Co, ^{58}Co, and ^{60}Co, are being presented. The experimental data are compared with calculations considering equilibrium as well as pre-equilibrium reactions according to the hybrid model of Blann. High energy part of the excitation functions is dominated by the pre-equilibrium reaction mechanism. Calculations were done using a priori calculational method of Overlaid Alice Code of Blann. Most of the excitation functions in the energy range mentioned above could be very well fitted with the hybrid model calculation for exciton number $n = 4$ with $n_p = 2$ and $n_n = 2$. The overall agreement with theory is good. Certain discrepancies, however, indicate the necessity to revise the hybrid model with respect to emission of complex particles.

Keywords. Cross-section; stacked foil technique; detector efficiency; isotope production; pre-equilibrium decay; overlaid alice code.

PACS No. 25·60

1. Introduction

The emission of forward-peaked hard component observed in the continuous spectra of light ejectiles and the high energy tails seen in the excitation functions of activation cross-sections induced by alpha particles, contains important information about the reaction mechanism. Several possible models have been proposed to explain the emission of non-compound energetic light particles (Griffin 1966; Harp et al 1968; Harp and Miller 1971; Blann 1971; Cline and Blann 1971) by the equilibration process from the nuclear system excited at medium energies. Prediction from these models as to the excitation functions and the energy spectra of the emitted particles compares well with the existing experimental data and reveals areas where the equilibrium statistical model is inadequate (Blann 1975a). More elaborate quantum mechanical theories (Agassi et al 1975; Tamura et al 1977; Tamura and Udagawa 1978; Feshback et al 1980) which are not applied to routinely measurable pre-equilibrium cross-sections have tended to support the foundations on which the classical models are built. This has prompted a continued interest in these models as tools both to predict the cross-section for a number of practical purposes and to test the adequacy of the underlying physics.

Considerable data is available on inclusive energy spectra of light ejectiles (Blann 1975a) and the complementary information on residual nucleus excitation functions

is far from being abundant. Regarding alpha-induced reactions the integral cross-section data exist only for a few target nuclei. The present work on alpha induced reactions on the target nuclei ^{181}Ta, ^{107,109}Ag and ^{59}Co is intended to supply data in the energy range up to 60 MeV.

In this paper several excitation functions for the reactions (i) ^{181}Ta(α, xn) $^{185-x}$Re, (ii) ^{107,109}Ag(α, ypxn) (iii) ^{59}Co-(α, ypxn) which were measured by using the stacked foil technique are presented. Theoretical calculations in the frame work of the equilibrium statistical model and the hybrid model were performed and the results compared with experimental excitation functions.

2. Experimental procedure

Excitation functions for the α-induced reaction on Ta, Ag and Co were obtained from the measurement of the residual activity of stacked foils. The stacks of commercially supplied foils of Ta, Ag and Co were irradiated in a specially constructed chamber as shown in figure 1. In this chamber, there is a facility to irradiate four stacks one after another just by rotating the top knob in 90° steps. The beam spot on the target was limited to 5 mm in diameter by using 10 cm long aluminium collimator in front of the targets. Stacks of about 10 to 20 foils with thickness $\simeq 25\,\mu$m in the case of Ta and Ag and $\simeq 50\,\mu$m in the case of Co were exposed to the unanalyzed external beam from 224 cm variable energy cyclotron at our Centre in Calcutta. The beam currents on the targets were kept between 0·5 and 1·0 μA. The total α-particle flux was measured with the help of the ORTEC current integrator. In addition, Al-flux monitoring foils were also kept in front of most of the stacks. The reason for using Al foils for flux monitoring is that the cross-section for the production of ^{22}Na and ^{24}Na from Al is very well known (Michel and Brinkmann 1980). Thus the reliability of absolute cross-section measurements is high. The unanalyzed beam energy resolution was $\simeq 0.2$ MeV. The accuracy is absolute energy is expected to be ± 2.0 MeV.
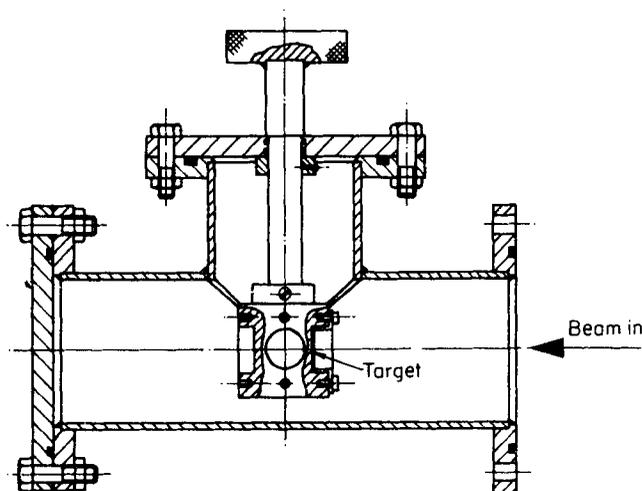

Figure 1. Target chamber.

In all the irradiations the beam energy was degraded down in the stacks to around 15 MeV. Hence, a few remarks on the applicability of the stacked foil method in these cases might be helpful to understand the loss of beam intensity, the energy straggling and the disturbing background due to secondary reactions when the beam is travelling through a large amount of material. The decrease of beam intensity I_x as a function of the transversed foil thickness x (cm) is given by the expression

$$I_x = I_0 \exp(-N\sigma x)$$

assuming a constant reaction cross-section σ. The quantity N(atoms/cm^3) in the case of an element of atomic weight A and density ρ gram per cm^3 is given by $N = (\rho/A)N_0$. For a compound of molecular weight M and density ρ, the quantity N is given as summation of the N_i of atoms of the ith kind per cm^3

$$N = \Sigma N_i = \Sigma(\rho N_0/M)\gamma_i,$$

where γ_i is the number of atoms of the kind i in a molecule of the compound and N_0 is Avagadro number ($0\cdot6022 \times 10^{24}$). For $\sigma = 2$ barn the maximum beam loss at the end of Ta stacks is always $< 0\cdot3\%$ and hence was neglected. The energy straggling at the end of the stacks is always much smaller than the energy loss of the beam in target foils. Hence the width of the folded energy distribution is not increased much. In reactions with the stack material the incoming beam will release a large amount of low energy ($E \leqslant 10$ MeV) neutrons and protons which can further react with the targets in stacks and disturb the yield mainly through (n, p), (n, α), (p, n) and (α, p) reactions. However the perturbative yields are mostly negligible.

The mean beam energy in each foil of a homogeneous or inhomogeneous stacked foil assembly can be calculated from the energy degradation of the initial beam energy according to the given stopping power values for the different materials. We have used the tabulated values of Williamson *et al* (1966) which are based on the experimentally well-known stopping power data for ^{27}Al. The average foil thickness of the stacks was determined by weighing punched out foils of 12·5 mm to 30 mm diameter. Though the method itself is rather accurate systematic deviations due to defects of the rim of the foil may occur. This could lead to underestimation of the thickness in the middle of the foil where the beam hits.

The nuclear data necessary for the evaluation of the cross section are presented in table 1. The half-lives were taken from the chart of nuclides (Eggbert *et al* 1981), the γ energies and branching ratios are taken from the table of isotopes by Lederer and Shirley (1978).

The γ rays emitted by the activated foils were measured with 114 c.c. Ge(Li) or HPGe detectors available at our Centre (VECC). The efficiency calibrations of the detectors were made with a calibrated Eu-152 source obtained from the Radiochemistry Unit at VECC. To improve the interpolation of efficiency from measured energy points to the required energy points, the efficiency curve was fitted (by nonlinear least square method) to a function of the form

$$y = \sum_{n=1}^{6} a_n x^{n-1} + b_1 \exp(-\lambda_1 x) + b_2 \exp(-\lambda_2 x).$$

The fit improved the overall accuracy of the efficiency interpolation to better than

1%. The fit as shown in figure 2 between experimental data (x points) and theoretical curve (solid line) with the above functional form is excellent.

In table 1 only those γ-rays which were chosen for the calculation of cross-sections are listed. Also included in table 1 are reaction Q-values which however exclude cluster emission. Thus in the case of α emission 28·30 MeV will have to be added to the listed Q-values. Q-values were calculated by using the atomic mass table by Wapstra and Audi (1985).

2.1 *Experimental error*

In tables 2, 3 and 4 the experimental cross-sections for the reactions ^{181}Ta(α, xn), ^{107,109}Ag$(\alpha, xnyp)$ and ^{59}Co $(\alpha, xnyp)$ are presented along with absolute errors. The absolute errors consist of uncertainties due to target foil thickness ($\pm 1\%$), the beam current ($\pm 2\%$), the detector efficiency ($\pm 5\%$) and the analysis of the γ-ray spectra, generally ($\leqslant 2\%$). The uncertainties caused by the larger dimensions of the irradiation area and the edge effects contribute a 5% error to the average error of the α-induced reaction. The above mentioned average error values do not include the uncertainties of the nuclear data.

2.2 *Cross-section determination*

The number of observed decays $y(t)$ is related to the total number of decays during the measuring time t by $\bar{y}(t) = y(t)/\varepsilon(E_r)I_{abs}(E_r)$ where $\varepsilon(E_r)$ being the detector efficiency and $I_{abs}(E_r)$ is absolute γ-ray intensity per decay. Dead time of the analyser is
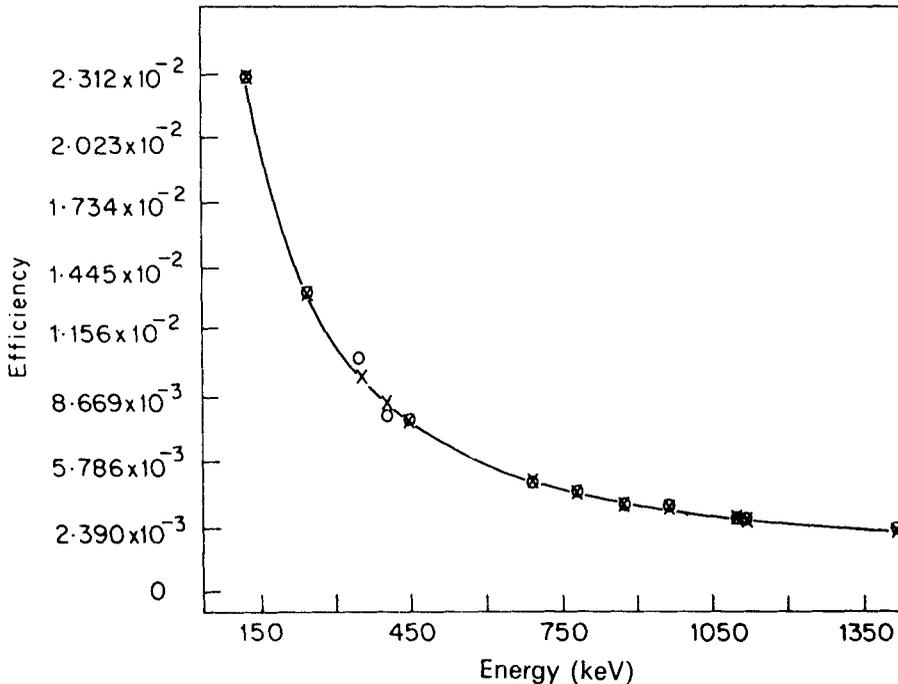

Figure 2. Nonlinear least-square fitted efficiency curve along with experimental values.

Table 1. Half-Lives γ-energies and branching ratios of the nuclides and
Q-valves reactions.

Nuclide	Half-Life	E_γ(keV)	I_γ(%)	Q-Value (MeV)	
^{181}Re	19·97 h	361	12·3	$(\alpha, 4n)$	$-31·75$
		366	57·0		
^{182}Re	64 h	229	26·84	$(\alpha, 3n)$	$-24·78$
		1121	21·3		
^{183}Re	71 d	162	23·0	$(\alpha, 2n)$	$-16·35$
^{184}Re	38 d	792	37·54	(α, n)	$-9·87$
^{111}In	2·81 d	171	94·2	$(\alpha, 2n)$	$-14·05$
		245	94·2		
^{105}Ag	41·3 d	344·5	42·71	$(\alpha, 2p4n)$	$-45·76$
^{54}Mn	312·2 d	834·81	99·97	$(\alpha, 4p5n)$	$-73·76$
^{56}Co	77·3 d	846·75	99·96	$(\alpha, 2p5n)$	$-58·76$
^{57}Co	270·0 d	122·07	85·5	$(\alpha, 2p4n)$	$-47·32$
^{58}Co	70·8 d	810·6	99·44	$(\alpha, 2p3n)$	$-38·74$
^{60}Co	5·272 y	1173·2	100·0	$(\alpha, 2pn)$	$-20·69$
		1332·5	100·0		

h = hours, d = days, y = years.

Table 2. Experimental cross-section for the α-induced reaction on Ta.

E_α (MeV)	Cross-section (mb)			
	^{184}Re	^{183}Re	^{182}Re	^{181}Re
57·5 ± 1·15	—	—	74·4 ± 6·7	325·2 ± 26·1
55·2 ± 1·2	—	—	74·83 ± 6·7	426·3 ± 34·2
52·8 ± 1·25	—	—	90·86 ± 7·3	598·4 ± 47·2
50·3 ± 1·3	—	—	108·55 ± 8·7	815·1 ± 65·2
47·7 ± 1·3	6·96 ± 0·7	75·6 ± 6·1	135·83 ± 10·9	988·6 ± 79·1
45·1 ± 1·35	8·71 ± 0·9	93·7 ± 7·5	190·01 ± 15·2	940·6 ± 75·3
42·4 ± 1·5	8·97 ± 0·9	125·6 ± 10·1	324·02 ± 25·9	745·6 ± 59·7
39·4 ± 1·5	10·22 ± 1·0	183·2 ± 14·6	550·05 ± 44·0	387·5 ± 31·0
36·4 ± 1·6	9·25 ± 0·9	263·9 ± 21·1	711·85 ± 57·0	87·9 ± 7·0
33·2 ± 1·7	14·92 ± 1·5	499·7 ± 4·0	595·0 ± 47·6	—
29·8 ± 1·75	18·4 ± 1·8	903·2 ± 72·2	363·4 ± 29·0	—
26·3 ± 1·9	24·93 ± 2·5	1061·3 ± 85·0	49·48 ± 4·5	—
22·5 ± 2·1	43·06 ± 4·3	647·3 ± 51·8	—	—
18·3 ± 2·1	19·79 ± 2·0	34·5 ± 2·8	—	—

Table 3. Experimental cross-section for the α-induced re-
action on silver.

	Cross-section (mb)	
E_α(MeV)	^{109}Ag(α, 2n)^{111}In	Ag(α, 2p4n)^{105}Ag
54·6 ± 0·95	42·5 ± 3·4	85·4 ± 6·8
52·8 ± 0·95	45·4 ± 3·6	83·5 ± 6·7
50·9 ± 0·95	52·0 ± 4·2	91·8 ± 7·4
49·0 ± 1·0	60·5 ± 4·9	132·2 ± 10·6
47·0 ± 1·0	64·2 ± 5·2	152·3 ± 12·2
45·0 ± 1·05	84·2 ± 6·7	146·3 ± 11·7
42·9 + 1·05	93·5 + 7·5	128·51 + 10·3
40·8 + 1·1	123·0 + 9·8	97·9 + 7·8
38·6 ± 1·1	172·0 ± 13·8	63·9 ± 5·2
36·2 ± 1·15	273·0 ± 21·8	31·3 ± 2·5
33·9 ± 1·25	459·8 ± 36·8	8·5 ± 0·9
31·4 ± 1·3	778·8 ± 62·3	—
28·8 ± 1·4	1087·0 ± 87·0	—
26·0 ± 1·5	1127·5 ± 90·2	
23·0 ± 1·6	875·0 ± 70·0	
19·8 ± 1·6	345·5 ± 27·6	
16·6 ± 1·6	10·7 ± 1·1	

Table 4. Experimental cross-section for the α-induced reaction on Co.

	Cross-section (mb)				
E_α(MeV)	Co(α4p5n)Mn	Co(α2p5n)Co	Co(α2p4n)Co	Co(α2p3n)Co	Co(α2pn)Co
54·5 ± 1·9	32·97 ± 2·64	39·48 ± 3·2	138·7 ± 11·2	120·44 ± 9·68	72·46 ± 5·84
50·7 ± 2·0	34·48 ± 2·76	19·66 ± 1·6	183·44 ± 14·7	111·83 ± 8·96	79·40 ± 6·4
46·7 ± 2·1	25·49 ± 2·04	3·88 ± 0·31	205·32 ± 16·5	120·18 ± 9·62	76·27 ± 6·16
42·5 ± 2·25	10·63 ± 0·86	0·17 ± 0·026	184·03 ± 14·7	162·70 ± 13·02	54·67 ± 4·4
38·0 ± 2·45	1·76 ± 0·02	0·17 ± 2·026	101·39 ± 8·2	228·07 ± 18·24	27·84 ± 2·32
33·1 ± 2·65	—	—	7·12 ± 0·6	224·41 ± 18·0	2·82 ± 0·24
27·8 ± 2·85	—	—	—	93·96 ± 7·5	—

automatically corrected by counting in lifetime mode. The corresponding reaction
yield N_0 is given for simple decays by

$$N_0 = \bar{y}(t) \exp(\lambda t_2)/[[1 - \exp(-\lambda t)] * [1 - \exp(-\lambda t_1)]/\lambda t_1],$$

where $\lambda = \ln 2/T_{1/2}$ is the decay constant and t_1 and t_2 are the length of the irradiation

time and the time between the end of the irradiation and the beginning of the measurement, respectively. In the case where $T_{1/2} \gg t_1, t$ the above relation becomes $N_0 = \bar{y}(t) \exp(\lambda t_2)/\lambda t$. N_0 is related to the cross-section σ by $N_0 = \sigma * (N_A \delta x) * I$ where N_A is the number of atoms/cm^3 of the target material, δx is the thickness of the target (in cm) and I is the number of particle/cm^2 for the total irradiation time.

3. Experimental results

3.1 *Integral excitation function for α-induced reaction on tantalum*

In table 2 and figures 3 to 6 our experimental results for the production of ^{184}Re, ^{183}Re, ^{182}Re and ^{181}Re radionuclides via α-induced reactions on ^{181}Ta are summarized. The errors given for the energy values include those of the thickness of the target foils, energy straggling as well as beam energy resolution (± 0.2 MeV). The range energy relation of the projectile in foil stack is taken from the tables of Williamson *et al* (1966).

Two details concerning the identification of the residual nuclei should be mentioned. The ^{182}Re nucleus, formed by $(\alpha, 3n)$ reaction, has a 13-hour isomeric and a 64-hour ground state. Before counting the sample the 13-hour isomeric state is allowed to decay completely. The reported cross-section of $(\alpha, 3n)$ excitation function is only for the ground state. The cross-section of the $(\alpha, 4n)$ excitation function was obtained by counting the 365 keV and 361 keV γ-rays together to reduce the uncertainties in extracting the individual peak areas.

So far, only a few experimental data concerning α-induced reactions exist in literature. Hermes *et al* (1974) from Bonn investigated the reaction ^{181}Ta(α, xn) in the energy range $E = 15-104$ MeV and $x = 2 \cdots 8$. They compared their results to equilibrium statistical model calculations using a Monte Carlo method. Recently Ernst *et al* (1982) also from Bonn investigated the α-induced reactions on tantalum ^{181}Ta$(\alpha, xnyp)$ in the energy range $E = 66-169.2$ MeV, $x \leqslant 12, y \leqslant 4$. These authors
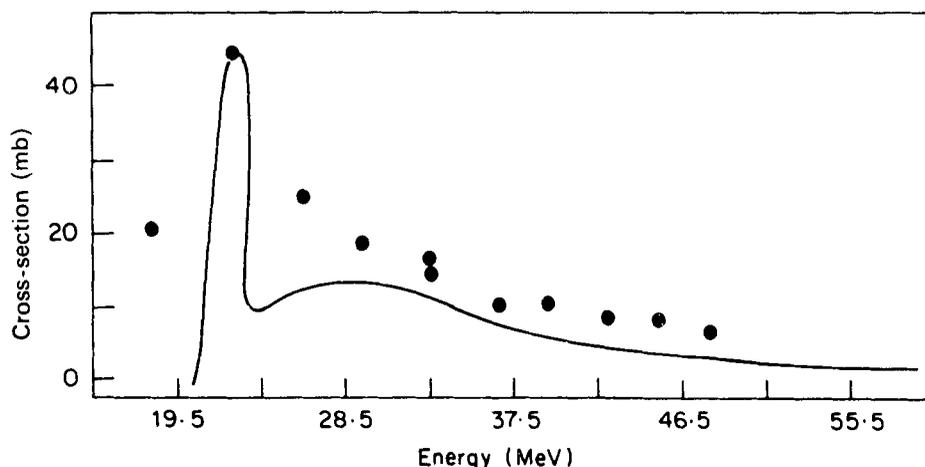
Figure 3. Experimental ^{181}Ta$(\alpha, n)^{184}$Re excitation function.

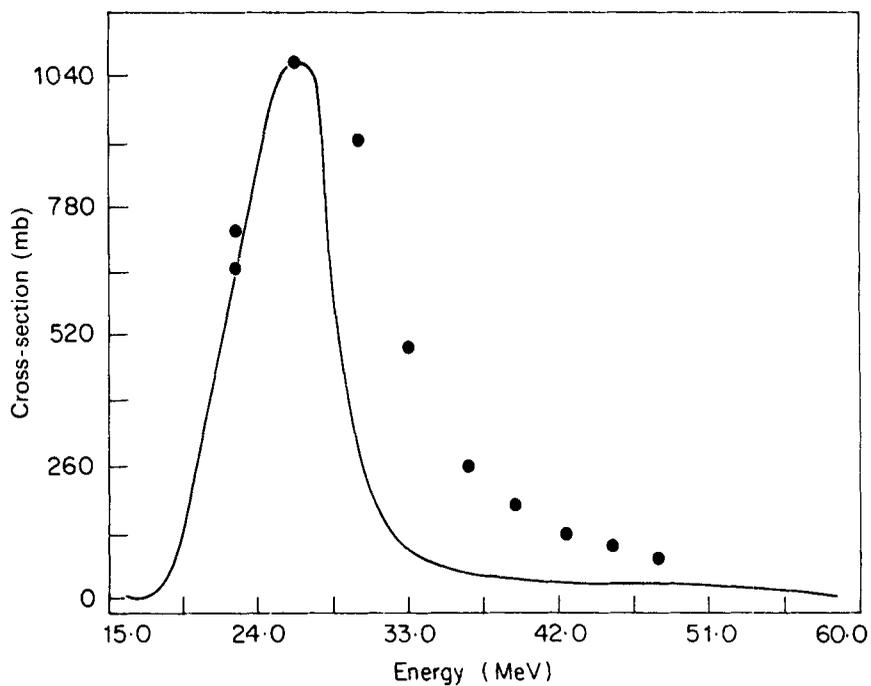**Figure 4.** Experimental ^{181}Ta$(\alpha, 2n)^{183}$Re excitation function.

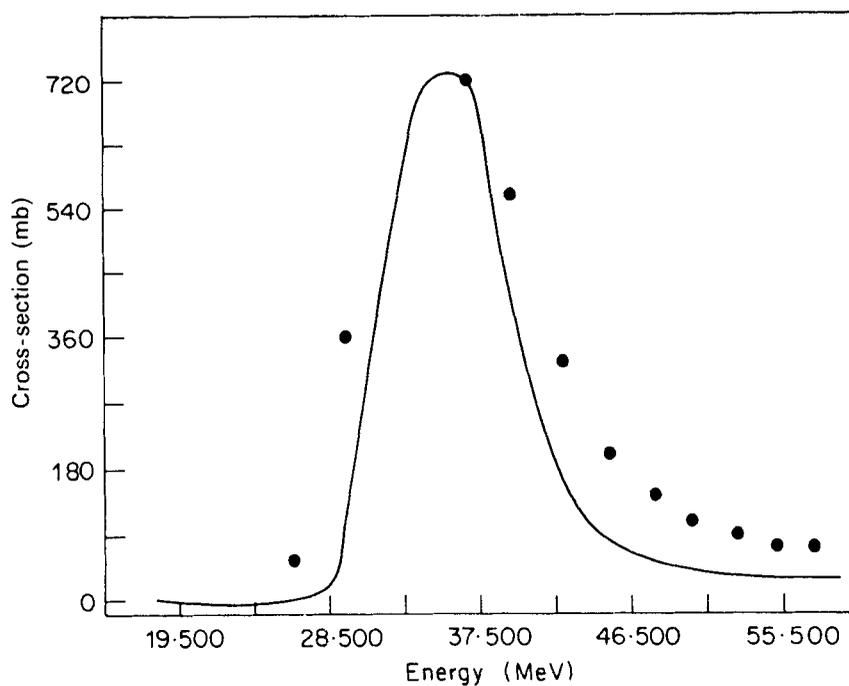**Figure 5.** Experimental ^{181}Ta$(\alpha, 3n)^{182}$Re excitation function.

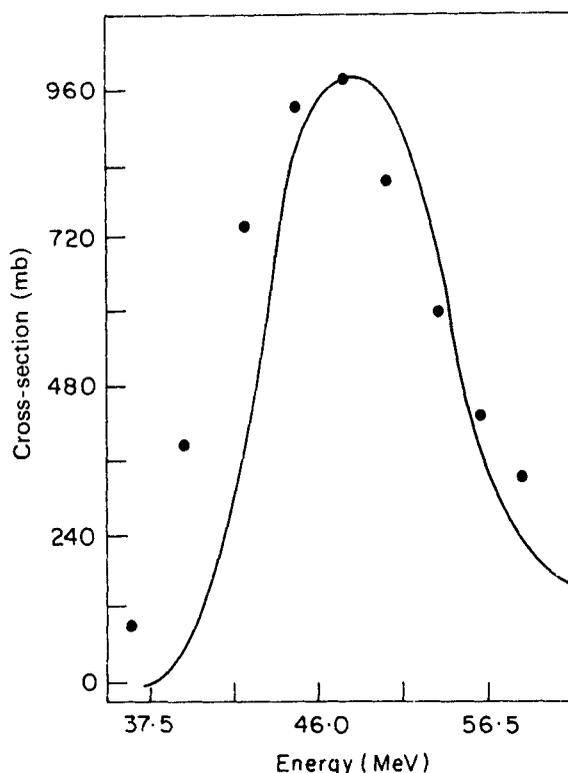**Figure 6.** Experimental ^{181}Ta$(\alpha, 4n)^{181}$Re excitation function.

have not measured ^{187}Ta(α, n) ^{184}Re cross-section, and they have published the total cross-section for 13 hour isomeric and 64 hour ground state for ^{181}Ta$(\alpha, 3n)$ ^{182}Re reaction whereas we have measured the cross-section corresponding to 64 hour ground state decay. For the remaining two reactions ^{181}Ta$(\alpha, 2n)$ ^{183}Re and ^{181}Ta$(\alpha, 4n)$ ^{181}Re the agreement is good in overlapping regions.

3.2 Integral excitation function for α-induced reaction on silver

In table 3 and figures 7 and 8 our experimental results for the production of radionuclides via α-induced reactions on ^{107,109}Ag are summarized. The errors given for the cross-sections are absolute errors, the uncertainties quoted for the energy values include those of the thickness in the target foils, energy straggling as well as beam energy resolution (± 0.2 MeV).

Up to now, only a few experimental data concerning α-induced reaction of ^{107,109}Ag exist in the literature. After the preliminary studies of Tendam and Brazdt (1947), Goshal (1948) and Bleuler et al (1953) studied the (α, n) and $(\alpha, 2n)$ reaction up to an alpha energy of 18 MeV. Porges (1956) obtained the excitation functions for the $(\alpha, 2n)$ and $(\alpha, 3n)$ reactions up to 40 MeV. Bishop et al (1964) reported the isomeric cross-section ratio for the $(\alpha, 3n)$ reaction. However, the experimental results do not agree with each other. Fukushima et al (1963) investigated the (α, n), $(\alpha, 2n)$ and $(\alpha, 3n)$ reactions on ^{109}Ag up to 40 MeV comparing the experimental cross-sections with
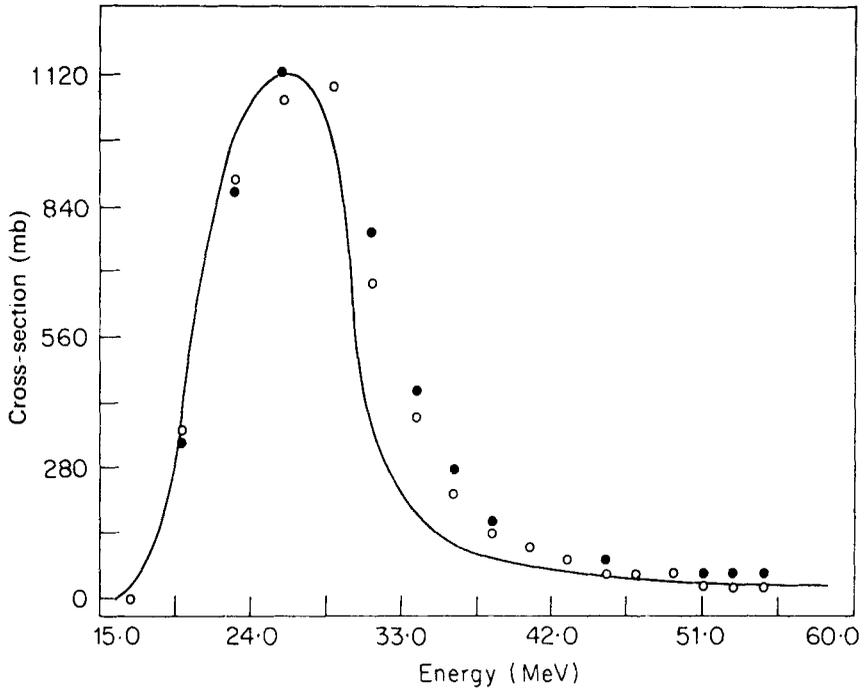
Figure 7.   Experimental ^{109}Ag$(\alpha, 2n)^{111}$In excitation function.

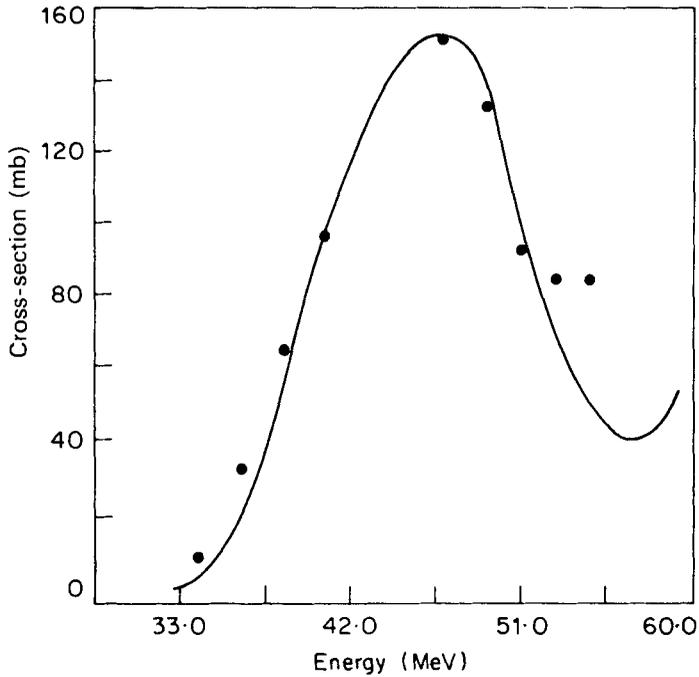**Figure 8.**   Experimental ^{109}Ag$(\alpha, 2p4n)^{105}$Ag excitation function.

the prediction of the statistical theory. The (α, n) reaction was measured by using enriched ^{109}Ag targets. The $(\alpha, 2n)$ and $(\alpha, 3n)$ measurements were performed by using natural silver target in the same series of experiments. Their absolute cross-section fits exactly into our excitation function. More recently Misaclides and Munzel (1980) measured the excitation function for the α-induced reaction with ^{107,109}Ag target in the energy range of 10–100 MeV. The experimental data were compared with the calculated values obtained by means of a hybrid model calculations. However, they have not published the data on ^{109}Ag($\alpha, 2n$) ^{111}In reaction and they have also not measured the ^{107}Ag($\alpha, 2p4n$) ^{105}Ag reaction. Therefore comparison between their data and our data could not be done.

3.3 *Integral excitation function for α-induced reaction on cobalt*

In table 4 and figures 9 to 13 our experimental results for the production of ^{54}Mn, ^{56}Co, ^{57}Co, ^{58}Co, and ^{60}Co radionuclides via α-induced reactions on ^{59}Co are summarized. Similar to the results on Ta and Ag the errors given for the cross-section are absolute errors and the uncertainties quoted for the energy values include those of the thickness of the target foils, energy straggling as well as beam energy resolution. Neuzil and Lindsay (1963) investigated the reaction ^{54}Co(α, α^3He) at fixed energies of 36·8 and 40·5 MeV. Zhukova *et al* (1972) studied the α-induced reaction on ^{59}Co for α-energies from 5·9 to 36·3 MeV. They reported production cross-section for the reactions $(\alpha, xn)x = 1, 2, 3$) and $(\alpha, 2pxn), x = 0, 3, 4$) in 1980. Michel and Brinkmann (1980) investigated ^{59}Co($\alpha, xnyp$), $x \leqslant 10, y \leqslant 11$ in the energy range $E = 20 - 172·5$ MeV. The absolute cross-sections of Zhukova, Michel and their coworkers do not agree with each other. Our absolute cross-sections, however, agree with the reported values of Michel and Brinkmann (1980) within the quoted error in the overlapping region of energies.

3.4 *Cross-section from Al foils*

Since the reaction ^{27}Al($\alpha, 4p3n$) ^{24}Na had been studied extensively in the past (Michel and Brinkmann 1980 and references 13–20 therein), we have checked the quality of our absolute cross-section values by measuring the cross-sections for this reaction by
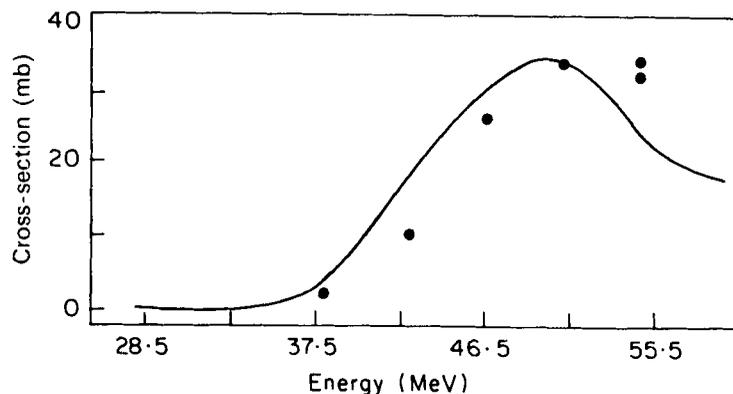

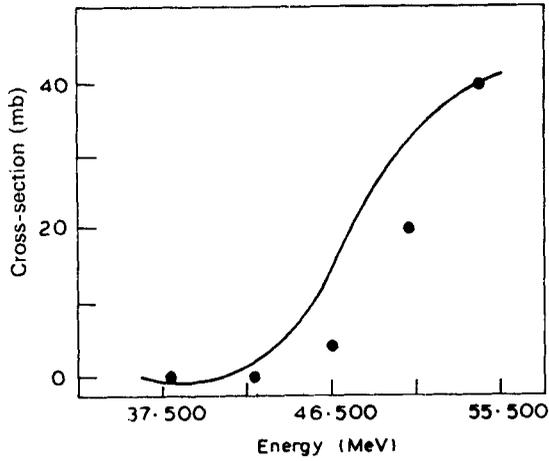**Figure 9.** Experimental ^{59}Co($\alpha, 4p5n$)^{54}Mn excitation function.

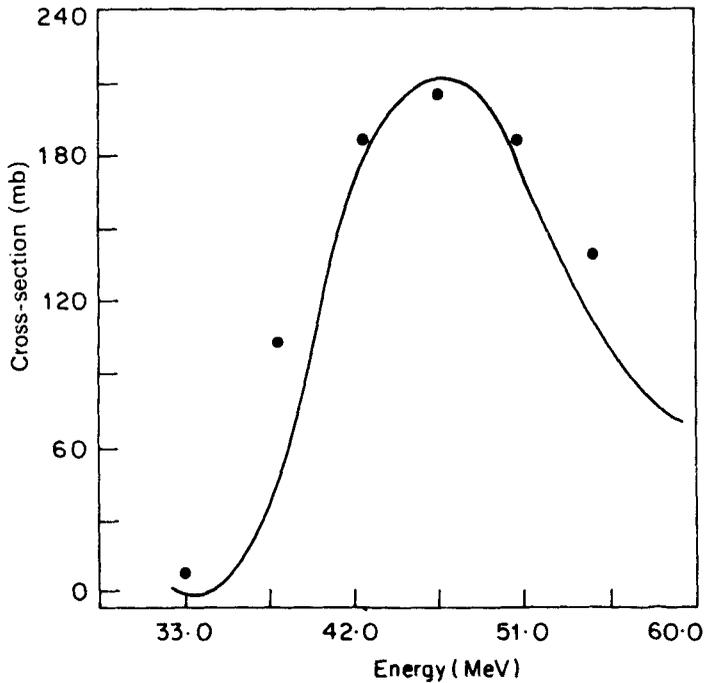**Figure 10.** Experimental ^{59}Co$(\alpha, 2p5n)^{56}$Co excitation function.

Figure 11. Experimental ^{59}Co$(\alpha, 2p4n)^{57}$Co excitation function.

way of flux monitoring foils kept in front of some of the stacks. A comparison of the production cross-section for ^{24}Na from α-bombardment with other authors shows good agreement. Our values for the cross-section at two alpha energies $E = 48.9 \pm 1.1$ MeV and 55.5 ± 1.0 MeV are $\sigma(48.9 + 1.1) = (4.24 \pm 0.21)$ mb and $\sigma(55.5 \pm 1.0) = (12.81 \pm 0.72)$ mb.
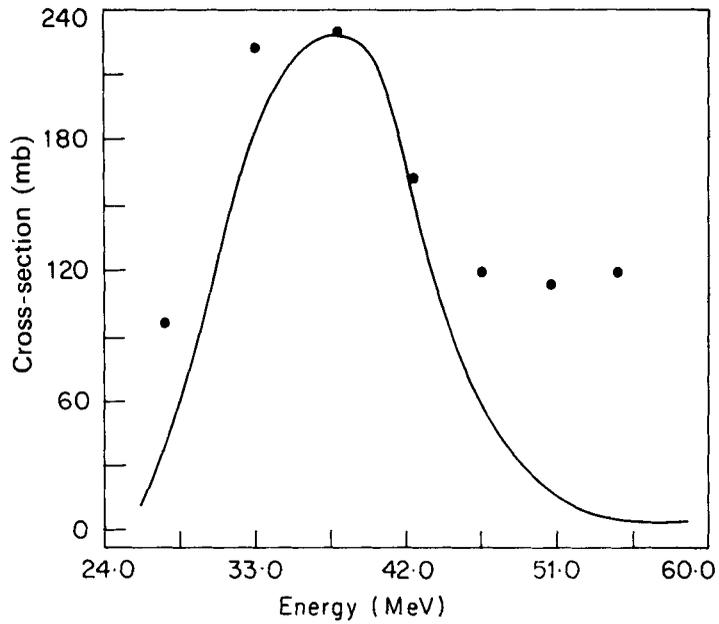
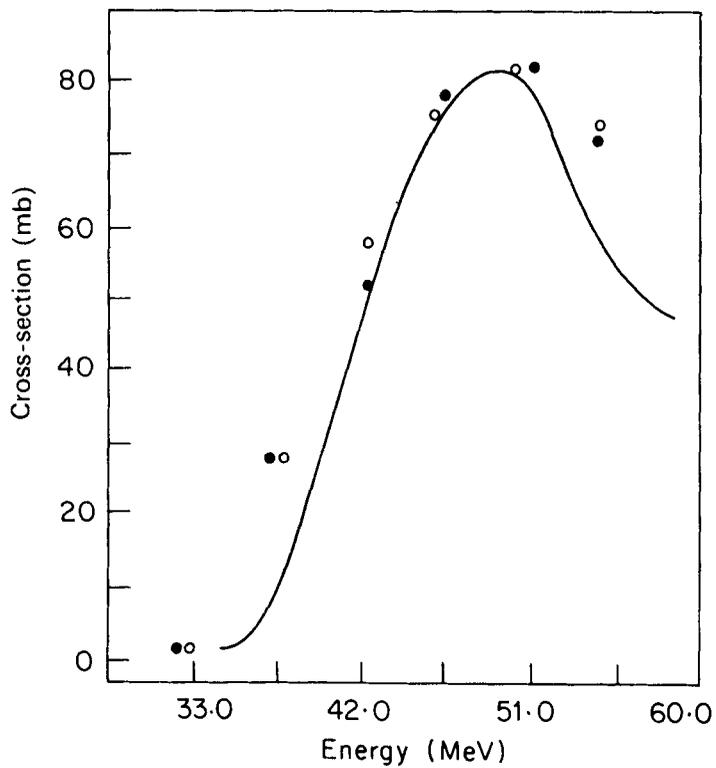**Figure 12.** Experimental ^{59}Co(α, 2p3n)^{58}Co excitation function.

Figure 13. Experimental ^{59}Co(α, 2pn)^{60}Co excitation function.

4. Comparison with theoretical prediction

Integral excitation functions of α-induced reactions have been discussed by several authors considering the models of the compound nucleus as well as of the pre-equilibrium reactions. They conclude that the theory of pre-equilibrium reactions is helpful in explaining the mechanism of α-induced reactions. In the present work our excitation functions are calculated on the basis of the hybrid-model (Blann 1971) using the program Overlaid Alice (Blann 1975b) on IRIS-80 computer at VECC. The calculations were done in 2 MeV steps from 10 to 60 MeV. Special emphasis was laid on testing the capability of the model to predict excitation functions from the known facts of nuclear matter using the *a priori* calculation methods of Overlaid Alice (Blann 1975b). Since the program system and the theories involved have been discussed by several authors, we confine ourselves to outlining the main points of preequilibrium theories. Some of the hybrid model are described in appendix 1.

The statistical part of the overlaid Alice can account for a large variety of reaction types. Besides evaporation of neutron and protons (Bohr and Wheeler 1939), clusters such as deuteron and α-particles can be considered. The nuclear masses were calculated from the Meyer and Swiatechi mass formula (Mayer and Swiatechi 1966, 1967) considering shell corrections as well as pairing corrections. The inverse cross-sections were calculated using the optical-model subroutine of Overlaid Alice, whereas the optical model parameters are those of Bechetti and Greenlees (1969). There are three main points of discussion when using the hybrid model option of Overlaid Alice: (i) the initial exciton configuration, (ii) the intranuclear transition rate and (iii) the so-called mean free path multiplier. In most of our calculations we have kept the initial exciton configuration as $n_0 = 4$, $n_p = 2$, $n_n = 2$. In the *a priori* formulations of the hybrid model, the intranuclear transition rates are calculated either from imaginary part of the optical model or from the free nucleon-nucleon scattering cross-section. But for particle energies exceeding 55 MeV the optical model parameters of Becchetti and Greenlees (1969) are no longer applicable and thus at higher energies the mean free path for intranuclear transition must be calculated from nucleon-nucleon scattering cross-sections. However, we have used only the latter option for calculating intranuclear transition rates. The mean free path multiplier K which is a kind of a free parameter and which was originally introduced by Blann to account for the transparency of nuclear matter should become unity. The solid lines in figure 3 to figure 13 show the hybrid model calculation for exciton $= 4$, $n_p = 2$ and $n_n = 2$. The $(+)$ and $(\times)$ points are the experimental data. The theoretical values are normalized to experimental data at the maximum cross-section point. For ^{181}Ta(α, n) ^{184}Re, (figure 3) the hybrid model fits the high energy tail very well where the lower energy part does not fit at all. On the other hand ^{59}Co$(\alpha, 2p3n)$ ^{58}Co (figure 12) the hybrid model fits the lower energy part very well whereas the high energy tail is not fitted at all. Aside from these two excitation functions the hybrid model fits all other excitation functions very well taking into account its limitations (see appendix 2).

5. Conclusions

A consistent set of 11 excitation functions has been measured for α-induced reactions with natural Ta, Ag and Co. The reliability of the mostly known cross-sections was

checked by inter-comparison with other measurements and by relating these to the well-known α-induced reactions on [27]Al. The comparison of the experimental data with results of the hybrid-model calculations shows a surprising agreement without any parameter adjustment for individual product: Pronounced pre-equilibrium effects of nucleons have been observed for most of the reactions. The excitation function for [59]Co(α, 2p3n)[58], however, could be explained by taking complex particle emission into account as well as by revising the hybrid model in this respect.

Acknowledgements

Appendix 1. Hybrid model for pre-equilibrium

The model proposed by Blann (1971) provides in some way a marriage between the simple exciton model proposed by Griffin (1966) and the more elaborate master-equation approach due to Harp and co-workers (Harp *et al* 1968; Harp and Miller 1971). This model predicts the probability of emission of a particle of type γ in the channel energy range ε to $\varepsilon + d\varepsilon$ as

$$P(\varepsilon)\,d\varepsilon = \sum_{n=n_0}^{\bar{n}} nP_\gamma[N_n(\varepsilon,u)/N_n(E)]*g\,d\varepsilon$$

$$*[\lambda_c(\varepsilon)/(\lambda_c(\varepsilon) + \lambda_{n+2}(\varepsilon))]*D_n,$$

where nP_r is the number of particles of type γ in an n-exciton state (where the exciton number means the number of excited particle plus hole) $N_n(\varepsilon,u)$ is the number of ways n excitons can be arranged such that one exciton, if emitted would have channel energy ε, leaving a residual excitation of $u = E - B_r - \varepsilon$ distributed between the other $n - 1$ excitons. The quantity $N_n(E)$ represents a total number of combinations of n particles plus holes at excitation E. The quantity in the first set of square brackets represents the fraction of the n-exciton states having one exciton at energy ε with respect to the continuum. The limiting value of the emission probability as defined by the above equation, integrated over all particle emission energy for a particular state with nP_r particles is not unit but nP_r i.e. the total number of excited particles.

Also in the above equation the emission rate into the continuum $\lambda_c(\varepsilon)$ of the particle at excitation ε is given by

$$\lambda_c(\varepsilon) = \sigma_r v\rho_c/g_r V,$$

where σ_r is the inverse cross-section and v the velocity of the particle having a density of state in the continuum, and a single-particle density of state g_r in the nucleus, V is an arbitrary volume cancelled by the same volume in ρ_c. The last factor D_n represents the fraction of the initial population surviving de-excitation by particle emission prior to the n-exciton state under consideration i.e. prior decay depletion factor.

The internal transition rate $\lambda n + 2$ of an excited particle at energy $\varepsilon + B_r$ above the Fermi energy has been based on calculated mean free path (Kikuchi and Kawai 1968)

in nuclear matter which however can be calculated either from nucleon-nucleon scattering cross-section or from imaginary part of the optical model. These methods are briefly summarized here.

(i) Intranuclear transition rates from nucleon-nucleon scattering cross-section: Nucleon-nucleon scattering cross-section at energy ε may be represented in terms of $B = v/c$ as (Kikuchi and Kawai 1968)

$$\sigma_{nn} = \sigma_{pp} = 10.63\,\beta^{-2} - 29.93\,\beta^{-1} + 42.9\,\text{mb},$$

$$\sigma_{np} = 34.10\,\beta^{-2} - 82.2\,\beta^{-1} + 82.2\,\text{mb}.$$

An effective cross-section σ may be calculated for scattering in nuclear matter with all collisions forbidden which would leave either scattered nucleon with less than the Fermi energy E_f. Kikuchi and Kawai present a result for such a calculation in terms of a parameter $P(X)$, where X is the ratio of Fermi energy to the energy the particle would have outside the nucleus plus the well depth V;

$$\bar{\sigma}(E) = \sigma_{ij}(E)P(X); \quad X = E_f/(\varepsilon + V) = E_f/V.$$

The values of $P(X)$ are given reasonably well by the relationship

$$P(X) = 1.0 - (7/5)X \quad \text{for} \quad X \leqslant 1/2,$$

$$P(X) = 1.0 - (7/5)X + (2/5)X(2 - X^{-1})^{5/2} \quad \text{for} \quad X \geqslant 1/2.$$

The average effective cross-section in a nucleus of A nucleons and Z protons and for a nucleon of type i at energy E may then be given by

$$\langle \sigma(E) \rangle_i = [(A - Z)\bar{\sigma}_n(E) + Z\bar{\sigma}_p(E)]/A.$$

The mean free path (MFP) may be defined in terms of the nuclear matter density ρ as

$$\text{MFP}(E)_i = 1.0/\rho\langle \sigma(E) \rangle_i.$$

The rate of intranuclear transition $\lambda_{n+2}(\varepsilon)$ is given by dividing the nucleon velocity by the mean free path

$$\lambda_{n+2}(\varepsilon) = \frac{v}{\text{MFP}(\varepsilon)} = \rho\langle \sigma(\varepsilon) \rangle_i \left(\frac{2(\varepsilon + V)}{m} \right)^{1/2}.$$

(ii) Intranuclear transition rates from the imaginary optical potentials: The use of optical potential in calculating intranuclear transition rates for pre-equilibrium decay models offers distinct advantages at least in principle over the nucleon-nucleon scattering approach. Specifically, the parameters of the optical potential have been determined from the results and trends of a large body of experimental data. The mean free path values are therefore based on experimental measurements in nuclear matter as opposed to the extrapolation of free scattering cross-sections to the nuclear environment. Secondly the question of possible errors in the treatment in (i) above due to failure to consider recoil momentum effects is avoided by using the optical potential. Becchetti and Greenlees (1969) have analysed a large body of data to find a "best set" of optical model parameters for nucleon-induced reactions. They have

given an imaginary potential of the form

$$W(R) = -W_V f(r, R, a) + W_{SF} 4a \frac{d}{dr} f(r, R, a)$$

$$f(r, R, a) = 1 \cdot 0 / [1 \cdot 0 + \exp(r - R)/a]$$

for protons $r = 1 \cdot 32$ fm, $1 = 0 \cdot 51 + 0 \cdot 7(N - Z)/A$ fm $W_V = 0 \cdot 22 \varepsilon - 2 \cdot 7$ MeV or zero whichever is greater, and $W_{SF} = 11 \cdot 8 - 0 \cdot 25 \varepsilon + 12 \cdot 0 (N - Z)/A$ MeV or zero whichever is greater. For neutrons $r = 1 \cdot 26$ fm, $a = 0 \cdot 58$ fm, $W_V = 0 \cdot 22 \varepsilon - 1 \cdot 56$ MeV or zero, whichever is greater, and $W_{SF} = 13 \cdot 0 - 0 \cdot 25 \varepsilon - 12 \cdot 0 (N - Z)/A$ MeV or zero whichever is greater (Becchetti and Greenless 1969).

The mean free path at energy ε outside the nucleus is related to the imaginary potential $W = W(R)$, and the real potential V by

$$\text{MFP}(\varepsilon) = \hbar^2 [(\varepsilon + V) + \{(\varepsilon + V) + W^2\}^{1/2}]^{1/2}$$

$$\simeq \frac{\hbar}{W} \left[\frac{(\varepsilon + V)}{2m} \right]^{1/2}$$

and the internal transition rate is given as in (i) by dividing the particle velocity v by the mean free path

$$\lambda_{n+2} = \frac{v}{\text{MFP}(\varepsilon)} = \left[\frac{2(\varepsilon + V)}{m} \right]^{1/2} \bigg/ \left[\frac{\hbar}{W} \left(\frac{\varepsilon + V}{2m} \right)^{1/2} \right] \simeq \frac{2W}{\hbar}.$$

Appendix 2. Expected accuracy of calculation

After considering the multitude of uncertainties in pre-equilibrium calculations such as the range of equilibrium and pre-equilibrium reaction cross-section involved, and the parameters such as inverse reaction cross-sections and level densities etc Blann (1975) considered that a result which is within a factor of two of the experimental result in absolute cross-section and which generally has the correct spectral shape and variation of yield with excitation energy, is an encouraging result.

References

Agassi D, Weidenmuller H A and Mantzouranis G 1975 *Phys. Rep.* **22** 145
Becchetti F D and Greenlees F W 1969 *Phys. Rev.* **182** 1190
Bishop G T, Huizenga J R and Hunmel J P 1964 *Phys. Rev.* **B135** 401
Blann M 1971 *Phys. Rev. Lett* **27** 337
Blann M 1975a *Annu. Rev. Nucl. Sci.* **25** 123
Blann M 1975b Overlaid Alice: A nuclear evaporation code, University of Rochester Report COO-3494-29 (unpublished)
Bleuler E, Stebbin A K and Tendam D J 1953 *Phys. Rev.* **90** 460
Bohr N and Wheeler J A 1939 *Phys. Rev.* **56** 426
Cline C K and Blann M 1971 *Nucl. Phys.* **A172** 225
Eggbert W S, Pfenning G, Munzel H and Nebenius H K 1981 *Chart of nuclides* 5th edition (Karlsruhe: Kernforschungszentrum)

Ernst J, Ibowshi R, Klampil H, Machner H, Mayer-Kuckuk T and Shanz R 1982 *Z. Phys.* **A308** 301

Feshback H, Kerman A and Konnin S E 1980 *Ann. Phys. (N.Y.)* **125** 429

Fukushima S, Kume S, Okamura H, Otozai K, Sakamoto K, Yoshizawa Y and Hayashi S 1963 *Nucl. Phys.* **41** 275

Goshal S N 1948 *Phys. Rev.* **73** 417

Griffin J J 1966 *Phys. Rev. Lett.* **17** 478

Harp G D, Miller J M and Berne J B 1968 *Phys. Rev.* **165** 1166

Harp G D and Miller J M 1971 *Phys. Rev.* **C3** 1847

Hermes F, Nasper E W, Kurz H E and Mayer-Kuckuk T 1974 *Nucl. Phys.* **A228** 165

Kikuchi K and Kawai M 1968 *Nuclear matter and nuclear reaction* (Amsterdam: North Holland)

Lederer C M and Shirley V S 1978 *Table of isotopes* 7th edition (New York: John Wiley)

Mayer W D and Swiatechi W J 1966 *Nucl. Phys.* **81** 1

Mayer W D and Swiatechi W J 1967 *Ark. Fys.* **36** 343

Michel R and Brinkmann G 1980 *Nucl. Phys.* **A338** 167

Misaclides P and Munzel H 1980 *J. Inorg. Nucl. Chem.* **42** 937

Neuzil E F and Lindsay R H 1963 *Phys. Rev.* **131** 1697

Porges K G 1956 *Phys. Rev.* **101** 225

Tamura T, Udagawa T, Feng D H and Kaur K K 1977 *Phys. Lett.* **B68** 109

Tamura T and Udagawa T 1978 *Phys. Lett.* **B78** 189

Tendam D J and Brazdt H L 1947 *Phys. Rev.* **72** 1118

Wapstra A H and Audi G 1985 *Nucl. Phys.* **A432** 1

Williamson C F, Boujot J P and Picard J 1966, CEA-R 3042

Zhukova U A and Kanashevich V I 1972 *Yadi Fiz* **16** 240

Zhukova O A, Kanashevich V I, Lapyer S C and Chursion G P 1973 *Sov. J. Nucl. Phys.* **16** 134